

Welfen Laboratory Reports

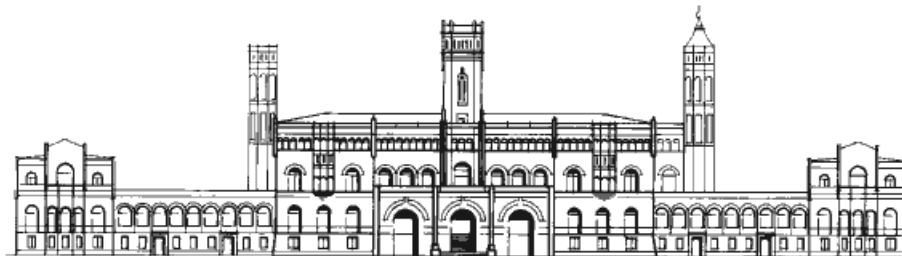
Editor: Franz-Erich Wolter

Welfen Laboratory, Report No. 2

Geodesic Voronoi Diagrams on Parametric Surfaces

Richard Kunze Franz-Erich Wolter Thomas Rausch

July 1997



Lehrstuhl Graphische
Datenverarbeitung
Welfenlabor
Institut für Informatik
Universität Hannover
Welfengarten 1
30167 Hannover, Germany

Division of Computer Graphics
and Geometric Modelling
Welfen Laboratory
Institute of Computer Science
University of Hannover
Welfengarten 1
30167 Hannover, Germany

few@informatik.uni-hannover.de
<http://www-c.informatik.uni-hannover.de>

Welfen Laboratory Reports No. 2

Franz-Erich Wolter (Editor)

Lehrstuhl Graphische Datenverarbeitung
Institut für Informatik
Universität Hannover
Welfengarten 1
30167 Hannover

3. Auflage
1st February 2000
(100 Stück)

Geodesic Voronoi Diagrams on Parametric Surfaces

Richard Kunze

Franz-Erich Wolter

Thomas Rausch

July 1997

Abstract

In this paper we will extend the concept of Voronoi diagrams to parameterized surfaces where distance between two points is defined as infimum over the lengths of surface paths connecting these points. We will present a method to compute Voronoi diagrams on these surfaces.

Keywords: Voronoi diagram, geodesic, parametric surface, computational geometry

1 Introduction and related works

The Voronoi diagram is one of the most fundamental data structures in computational geometry. The topic is well researched and understood, see [1] for an overview. However, most previous works deal with Voronoi diagrams in Euclidean or L_1 space, with exception of [4]. Klein looks at Voronoi diagrams from a different point of view, defining a *Voronoi region* as intersection of half-planes defined by a set of (almost) arbitrary curves and the Voronoi diagram as union of the borders of its regions.

In this paper, we will employ a divide and conquer scheme to calculate Voronoi diagrams on parametric surfaces. The crucial part is here to compute the Voronoi diagram of two points, i.e. their medial curve. Until recently, there were no proper tools available to achieve this goal. However, [6] fills this gap, providing us with the means to calculate the medial curve of two points on a parametric surface.

Possible applications include the generation of parameterization independent triangular meshes on parameterized surfaces. Since geodesic Voronoi diagrams as defined here depend only on the geometry of the surface and not on its parameterization, the dual geodesic Delaunay triangulation could be used as a basis for such a mesh.

2 Definitions and Background

Let $\mathbf{r}(u, v) = (x(u, v), y(u, v), z(u, v))^T$ be a regular parameterization of a given surface S and $I \subset \mathbb{R}^2$ its parameter domain. Let $p, q \in S$ be two points in parameter space of S and $\mathbf{r}(p)$, $\mathbf{r}(q)$ the corresponding surface points. Let $\mathcal{P}_{p,q}$ denote the set of all paths in S connecting $\mathbf{r}(p)$ and $\mathbf{r}(q)$. The distance $d(p, q)$ between $\mathbf{r}(p)$ and $\mathbf{r}(q)$ is defined as the infimum of lengths of all paths $c \in \mathcal{P}_{p,q}$.

If I is a closed rectangle and $\mathbf{r} : I \rightarrow S$ is C^2 -smooth, then there exists a minimal path $c_{\min} \in \mathcal{P}_{p,q}$ whose length equals $d(p, q)$. If c_{\min} stays away from the boundary of the surface patch $S = \mathbf{r}(I)$, then c_{\min} is a geodesic and satisfies the geodesic differential equation (2) (c.f. [8, 9, 10]). Since this property allows us to measure distances on S by computing the length of geodesics, we refer to $d(p, q)$ as *geodesic distance* between $\mathbf{r}(p)$ and $\mathbf{r}(q)$. Note that d defines a metric on both S and I , since

$$\begin{aligned} d(p, p) &= 0 \\ d(p, q) &= d(q, p) \\ d(p, q) &\leq d(p, r) + d(r, q) \end{aligned}$$

holds for all $p, q, r \in I$.

Let now $P = \{p_1, \dots, p_n\}$, $p_i \in I$ be a set of n distinct points in the parameter domain of \mathbf{r} . Let

$$\begin{aligned} M(p, q) &= \{z \in I \mid d(z, p) = d(q, z)\} \\ D(p, q) &= \{z \in I \mid d(z, p) < d(q, z)\} \end{aligned} \tag{1}$$

$M(p, q)$ is the *equidistantial set* of p and q . $M(p, q)$ divides I in two sub-regions; $D(p, q)$ is the region containing p . The set

$$D(p, P) = \bigcap_{\substack{q \in P \\ q \neq p}} D(p, q)$$

consists of all points $z \in I$ for which the geodesic distance between $\mathbf{r}(z)$ and $\mathbf{r}(p)$ is smaller than the geodesic distance to any other point $\mathbf{r}(q)$, $p \neq q \in P$. $D(p, P)$ is called the (*open*) *Voronoi region of p with respect to P* . The union

$$V(P) = \bigcup_{p \in P} \partial D(p, P)$$

of all region boundaries is called the *Voronoi diagram* of P . The common boundary of two Voronoi regions is a *Voronoi edge*. A point where two Voronoi edges meet is called a *Voronoi vertex*. For every Voronoi vertex z , there are at least three distinct points $p, q, r \in P$ for which $d(z, r) = d(z, p) = d(z, q)$ holds.

2.1 Geodesic Voronoi diagrams versus Euclidean Voronoi diagrams

The generalization of Voronoi diagrams on arbitrary surfaces shows some special problems which do not occur in the Euclidean case. The first problem arises in computing $M(p, q)$, the equidistantial set of two points. This is achieved easily in the Euclidean case, since here $M(p, q)$ is the straight line perpendicular bisecting the line segment that connects p and q . The tools needed to calculate $M(p, q)$ on parameterized surfaces are discussed in section 3.1.

Some further complications follow directly from $M(p, q)$ not being a straight line: If we employ a divide and conquer scheme to calculate the Voronoi diagram, we need to “sew up” the sub-diagrams obtained in the divide step. For this we need to compute the so called *bisector* of these two diagrams, the place where these sub-diagrams meet in the original diagram. In the Euclidean case, the bisector is made up of connected straight line segments and tends to infinity on both ends. This is not true in the case of arbitrary surfaces, making the problem of calculating this bisector a lot more difficult.

Even more problems arise due to the fact that $M(p, q)$ can be a periodic curve, see section 4 for an example.

2.2 General assumptions and constraints

Throughout this paper, we will assume that S is a surface patch, i.e. the parameter domain of S is a finite rectangle. This is not a serious restriction: Since $|P| < \infty$ we can circumscribe the interesting region of $V(P)$ by a finite rectangle and restrict our calculations to the resulting patch even if the parameter domain of S is infinite. We will assume also that the distance $d(p, q)$ between two surface points $\mathbf{r}(p)$ and $\mathbf{r}(q)$ can be computed by calculating the length of a geodesic connecting $\mathbf{r}(p)$ and $\mathbf{r}(q)$ (see also [5, 8, 9, 10]).

Furthermore, we assume that every edge of $V(P)$ for $|P| > 2$ starts and ends at either a Voronoi vertex or extends to the boundary of the parameter domain, thus preventing “isolated edges” or “islands” in $V(P)$ (see section 4, figure 6 for an example of a Voronoi diagram containing “islands”). Edges may start and end at the same point. Note that this restriction is weaker than requiring $M(p, q)$ to reach the border of the parameter domain for every $p, q \in P, p \neq q$.

3 Outline of the algorithm

3.1 Computing $M(p, q)$

In order to compute $M(p, q)$ on a parameterized surface, we need to employ several results and techniques from differential geometry that are too lengthy to introduce here from the very beginning. For basics in differential geometry, we refer to [3]. Throughout this paper, we will use $\mathbf{r}_u, \mathbf{r}_v, \mathbf{r}_{uu}, \mathbf{r}_{uv}, \mathbf{r}_{vu}$ and \mathbf{r}_{vv} to denote the first and second order partial derivatives of \mathbf{r} . In this section, we will only give a short introduction to the tools needed to compute $M(p, q)$ for two points p and q , see [6] for a thorough discussion of geodesic offsets and medial curves. We will however restate a well known theorem on geodesic curves, which allows us to calculate geodesics by means of a differential equation:

Theorem 3.1 *For every point p of a regular parameterized surface S and every vector $w \in T_p(S)$, $w \neq 0$ there exists an $\epsilon > 0$ and a unique geodesic curve $\gamma(s) \subset S$, $s \in (-\epsilon, \epsilon)$ with $\gamma(0) = p$ and $\gamma'(0) = w$. The curve $(u(s), v(s))$ in the parameter space of S with $\gamma(s) = \mathbf{r}(u(s), v(s))$ satisfies the system of differential equations:*

$$\left. \begin{aligned} u'' + \Gamma_{11}^1(u')^2 + 2\Gamma_{12}^1 u'v' + \Gamma_{22}^1(v')^2 &= 0 \\ v'' + \Gamma_{11}^2(u')^2 + 2\Gamma_{12}^2 u'v' + \Gamma_{22}^2(v')^2 &= 0 \end{aligned} \right\} \quad (2)$$

A proof of the theorem can be found in [3]. The coefficients Γ_{ij}^k in (2) are known as *Christoffel Symbols*. They are differentiable functions of the parameters u and v and can be obtained by solving the following system of linear equations:

$$\left. \begin{aligned} \left\{ \begin{aligned} \Gamma_{11}^1 E + \Gamma_{11}^2 F &= \langle \mathbf{r}_{uu}, \mathbf{r}_u \rangle \\ \Gamma_{11}^1 F + \Gamma_{11}^2 F &= \langle \mathbf{r}_{uu}, \mathbf{r}_v \rangle \end{aligned} \right. \\ \left\{ \begin{aligned} \Gamma_{12}^1 E + \Gamma_{12}^2 F &= \langle \mathbf{r}_{uv}, \mathbf{r}_u \rangle \\ \Gamma_{12}^1 F + \Gamma_{12}^2 F &= \langle \mathbf{r}_{uv}, \mathbf{r}_v \rangle \end{aligned} \right. \\ \left\{ \begin{aligned} \Gamma_{22}^1 E + \Gamma_{22}^2 F &= \langle \mathbf{r}_{vv}, \mathbf{r}_u \rangle \\ \Gamma_{22}^1 F + \Gamma_{22}^2 F &= \langle \mathbf{r}_{vv}, \mathbf{r}_v \rangle \end{aligned} \right. \end{aligned} \right\} \quad (3)$$

These equations are grouped into three pairs of independent equations each having the determinant $EG - F^2 \neq 0$, provided the surface parameterization \mathbf{r} is regular. Furthermore, these equations determine all Christoffel symbols since they are symmetric with respect to their lower indices, i.e. $\Gamma_{ij}^k = \Gamma_{ji}^k$. The coefficients E , F and G of the first fundamental form of \mathbf{r} are defined as

$$E := \langle \mathbf{r}_u, \mathbf{r}_u \rangle, \quad F := \langle \mathbf{r}_u, \mathbf{r}_v \rangle, \quad G := \langle \mathbf{r}_v, \mathbf{r}_v \rangle$$

$\langle \cdot, \cdot \rangle$ denotes the inner product.

3.1.1 Geodesic circles and offset functions

Definition 3.2 Let $p = \mathbf{r}(u, v) \in S$ be a point on a regular surface S . For every $t_0 \in [0, 2\pi)$ γ_{t_0} denotes the arc length parameterized geodesic curve emanating from p in direction $\cos t_0 \mathbf{r}_u + \sin t_0 \mathbf{r}_v$. The vectors \mathbf{r}_u , \mathbf{r}_v are the partial derivatives of \mathbf{r} . The set

$$\{\gamma_{t_0}(s) \mid t_0 \in [0, 2\pi)\}$$

is called the **geodesic circle** around p with radius s .

This notation has to be treated with some care. The distance between p and points on the geodesic circle of radius s as defined above may actually be less than s . Consider e.g. a point p on the unit sphere and the geodesic circle of radius $\frac{3\pi}{2}$ around p . The distance on S between points on this geodesic circle and p is $\frac{\pi}{2} < \frac{3\pi}{2}$. We know however that geodesics emanating from p will be shortest paths between p and the geodesic circle of radius s iff no pair of distinct geodesics $\gamma_{t_0}, \gamma_{t_1}$ emanating from p intersect before they reach this geodesic circle (c.f. [8, 10]).

Proposition 3.3 The geodesic circle around a given point p with radius s_0 can be represented as a parameterized curve $\alpha_{s_0}(t)$

Proof: Every point $\gamma_{t_0}(s_0)$ on the geodesic circle is the solution of the system of differential equations (2), which itself has a differentiable right hand side. By definition 3.2, the geodesic circle may be obtained by a differentiable variation of t . By a classical result of the theory of ordinary differential equations, the solution obtained by this variation is a differentiable function of t . ■

Note that geodesic circles need not be regular. For instance, consider the unit sphere and a geodesic circle with radius π . This geodesic circle consists solely of the antipodean point of p .

Definition 3.4 Let S be a regular parametric surface parameterized by $\mathbf{r}(u, v)$ and let p be a point on S . The function $\mathcal{O}_p : (s, t) \rightarrow (u, v)$ defined by

$$\mathbf{r}(\mathcal{O}_p(s, t)) = \gamma_t(s) = \alpha_s(t)$$

is called the **geodesic offset function** on S with respect to p .

By definition 3.4, $\mathcal{O}_p(s_0, t_0)$ yields the (u, v) -parameters of $\gamma_{t_0}(s_0)$, i.e. the point on the geodesic circle with radius s_0 and angle t_0 . Note that $\mathcal{O}_p(s_0, t_0)$ can be obtained by solving the geodesic differential equation (2).

Proposition 3.5 *The geodesic offset function is differentiable. Its partial derivatives $\partial_s \mathcal{O}_p$ and $\partial_t \mathcal{O}_p$ are given by*

$$\gamma'_{t_0}(s) = (\mathbf{r}_u, \mathbf{r}_v) \cdot \partial_s \mathcal{O}_p \quad (4)$$

$$\alpha'_{s_0}(t) = (\mathbf{r}_u, \mathbf{r}_v) \cdot \partial_t \mathcal{O}_p \quad (5)$$

where $(\mathbf{r}_u, \mathbf{r}_v)$ is the Jacobian matrix of \mathbf{r} .

Proof: The function $\mathcal{O}_p(s, t)$ is solution of the geodesic differential equations (2) with its initial values depending differentiably on s, t . Thus $\mathcal{O}_p(s, t)$ is a differentiable function. The equations above follow immediately by applying the chain rule. ■

By solving the geodesic differential equations we not only obtain the parameters $(u(s), v(s))$ of the geodesic curve $\gamma_{t_0}(s)$ as stated above, but also $(u'(s), v'(s))$ which equals the partial derivative $\partial_s \mathcal{O}_p$. With the following result we are able to compute $\partial_t \mathcal{O}_p$:

Proposition 3.6 *Let $\gamma_{t_0}(s)$ denote the arc length parameterized geodesic curve emanating from $p \in S$ at angle t_0 and $\alpha_s(t)$ be the parameterization of the geodesic circle with radius s around p . For every s_0, t_0 the tangent vectors $\alpha'_{s_0}(t_0)$ and $\gamma'_{t_0}(s_0)$ of the geodesic circle and the geodesic respectively are orthogonal to each other. The signed length $y_{t_0}(s) = \pm \|\alpha'_s(t_0)\|$ of the geodesic circle's tangent vector satisfies the ordinary differential equation*

$$y''_{t_0}(s) = -K(s)y_{t_0}(s)$$

where $K(s)$ denotes the Gaussian curvature of S at $\mathbf{r}(\mathcal{O}_p(s, t_0)) = \gamma_{t_0}(s)$.

A proof of this proposition can be found in [6]. Initial values for calculating y by numerically solving this differential equation are $y(0) = 0$, $y'(0) = 1$, see [2], p. 199–203 or [3] for a proof.

3.1.2 Medial curves

Exploiting proposition 3.6 we are able to derive an algorithm for computing the medial curve of two distinct points on a surface. Let p, q be two points on a parameterized surface S . The geodesic offset functions with respect to p and q shall be denoted $\mathcal{O}_p(s, t)$ and $\mathcal{O}_q(s, t)$. Consider the vector-valued function $\mathbf{F} : \mathbb{R}^3 \rightarrow \mathbb{R}^2$ defined by

$$\mathbf{F}(r, \varphi, \psi) := \mathcal{O}_q(r, \psi) - \mathcal{O}_p(r, \varphi)$$

Let (r_0, φ_0, ψ_0) be a triple satisfying

$$\begin{aligned} \mathbf{F}(r_0, \varphi_0, \psi_0) &= 0 \\ \det(\partial_r \mathbf{F}(r_0, \varphi_0, \psi_0), \partial_\psi \mathbf{F}(r_0, \varphi_0, \psi_0)) &\neq 0 \end{aligned} \quad (6)$$

According to the implicit function theorem, a neighborhood J of φ_0 and differentiable functions $r, \psi : J \rightarrow \mathbb{R}$ exist such that

$$\mathbf{F}(r(\varphi), \varphi, \psi(\varphi)) = 0$$

holds for every $\varphi \in J$. These functions induce a curve $\mathbf{m}(\varphi)$ in parameter space of S that has the property

$$\mathcal{O}_p(r(\varphi), \varphi) = \mathbf{m}(\varphi) = \mathcal{O}_q(r(\varphi), \psi(\varphi)) \quad (7)$$

for every $\varphi \in J$. The corresponding curve $\mathbf{r}(\mathbf{m}(\varphi)) =: \boldsymbol{\mu}(\varphi) \subset S$ satisfies

$$\gamma_{p,\varphi}(r(\varphi)) = \boldsymbol{\mu}(\varphi) = \gamma_{q,\psi(\varphi)}(r(\varphi)), \quad \varphi \in J$$

where $\gamma_{p,\varphi}$ and $\gamma_{q,\psi(\varphi)}$ are geodesics emanating from p and q in directions determined by angles φ and $\psi(\varphi)$ in the tangential planes $T_p(S)$ and $T_q(S)$ respectively. In other words: $\boldsymbol{\mu}(\varphi)$ lies at geodesic distance $r(\varphi)$ to both the points p and q where the distance is taken along the geodesic $\gamma_{p,\varphi}$ and $\gamma_{q,\psi(\varphi)}$ respectively. The condition of regularity in (6) in more detail is $\det(\partial_s \mathcal{O}_q - \partial_s \mathcal{O}_p, \partial_t \mathcal{O}_q) \neq 0$. Without loss of generality we can assume this holds for all $\varphi \in J$, maybe after reducing J . Differentiating equation (7) yields

$$(\partial_s \mathcal{O}_q - \partial_s \mathcal{O}_p, \partial_t \mathcal{O}_q) \begin{pmatrix} r' \\ \psi' \end{pmatrix} = \partial_t \mathcal{O}_p \quad (8)$$

and since the matrix is assumed to be regular for all $\varphi \in J$ we have

$$\begin{pmatrix} r' \\ \psi' \end{pmatrix} = (\partial_s \mathcal{O}_q - \partial_t \mathcal{O}_p, \partial_t \mathcal{O}_q)^{-1} \partial_t \mathcal{O}_p \quad (9)$$

This is a system of ordinary differential equations that can be used to trace $\mathbf{m}(\varphi)$, provided appropriate initial values can be found. The partial derivatives of \mathcal{O}_p and \mathcal{O}_q can be computed by means of the tools introduced in section 3.1.1.

If we would use equation (9) to trace $\mathbf{m}(\varphi)$, the resulting curve would be parameterized according to the angle φ of the geodesics emanating at p . This parameterization is somewhat unwieldy, making it especially difficult to estimate errors in approximations of $\mathbf{m}(\varphi)$. However, we are able to force \mathbf{m} to be parameterized by its arc length by introducing one additional condition in equation (7). This yields the following system of equations:

$$\left. \begin{aligned} \mathcal{O}_p(r(t), \varphi(t)) &= \mathbf{m}(t) = \mathcal{O}_q(r(t), \psi(t)) \\ \|\mathbf{m}'(t)\| &= \|\partial_s \mathcal{O}_p r' + \partial_t \mathcal{O}_p \varphi'\| = 1 \end{aligned} \right\} \quad (10)$$

By differentiating the first equation of (10) we get

$$\partial_s \mathcal{O}_p r' + \partial_t \mathcal{O}_p \varphi' = \partial_s \mathcal{O}_q r' + \partial_t \mathcal{O}_q \psi'$$

With $\partial_x \mathcal{O}_{p,i}$, $\partial_x \mathcal{O}_{q,i}$, $i = 1, 2$, $x \in \{s, t\}$ denoting the i -th component of these two dimensional vectors, the conditions above are equivalent to:

$$\left. \begin{aligned} (\partial_s \mathcal{O}_{q,1} - \partial_s \mathcal{O}_{p,1}) r' + \partial_t \mathcal{O}_{q,1} \psi' - \partial_t \mathcal{O}_{p,1} \varphi' &= 0 \\ (\partial_s \mathcal{O}_{q,2} - \partial_s \mathcal{O}_{p,2}) r' + \partial_t \mathcal{O}_{q,2} \psi' - \partial_t \mathcal{O}_{p,2} \varphi' &= 0 \\ \|\partial_s \mathcal{O}_p r' + \partial_t \mathcal{O}_p \varphi'\| &= 1 \end{aligned} \right\} \quad (11)$$

We assume that neither $\partial_t \mathcal{O}_p$ nor $\partial_t \mathcal{O}_q$ vanish for the considered medial point. By using the first two equations of (11) to eliminate ψ' and by introducing the abbreviations

$$\begin{aligned} D_1 &:= \det(\partial_t \mathcal{O}_p, \partial_t \mathcal{O}_q) \\ D_2 &:= \det(\partial_s \mathcal{O}_q - \partial_s \mathcal{O}_p, \partial_t \mathcal{O}_q) \\ D_3 &:= \det(\partial_s \mathcal{O}_q - \partial_s \mathcal{O}_p, \partial_t \mathcal{O}_p) \end{aligned}$$

we obtain the modified system

$$\left. \begin{aligned} r' &= \frac{D_1}{D_2} \cdot \varphi' \\ (\partial_s \mathcal{O}_{q,2} - \partial_s \mathcal{O}_{p,2}) r' + \partial_t \mathcal{O}_{q,2} \psi' - \partial_t \mathcal{O}_{p,2} \varphi' &= 0 \\ \|\partial_s \mathcal{O}_p r' + \partial_t \mathcal{O}_p \varphi'\| &= 1 \end{aligned} \right\} \quad (12)$$

Note that $D_2 \neq 0$ by assumption. Some straightforward calculations finally lead to the following system of differential equations, allowing us to trace $\mathbf{m}(t)$ parameterized by its arc length in parameter space:

$$\left. \begin{aligned} r' &= \pm \frac{D_1}{\|D_1 \partial_s \mathcal{O}_p + D_2 \partial_t \mathcal{O}_p\|} \\ \varphi' &= \pm \frac{D_2}{\|D_1 \partial_s \mathcal{O}_p + D_2 \partial_t \mathcal{O}_p\|} \\ \psi' &= \pm \frac{D_3}{\|D_1 \partial_s \mathcal{O}_p + D_2 \partial_t \mathcal{O}_p\|} \end{aligned} \right\} \quad (13)$$

The sign in (13) must be chosen according to $\text{sign}(\varphi') = \pm \text{sign}(D_2)$.

Note that φ and ψ are angles in the tangent planes $T_p(S)$ and $T_q(S)$ respectively. Corresponding directions (u_ϕ, v_ϕ) , $\phi \in \{\varphi, \psi\}$ in parameter space are obtained by applying the transformation

$$\begin{aligned} u_\phi &= \frac{\cos \phi - \frac{F}{\sqrt{EG - F^2}} \sin \phi}{\sqrt{E}} \\ v_\phi &= \frac{\sin \phi}{\sqrt{EG - F^2}} \end{aligned}$$

where $E = \langle \mathbf{r}_u, \mathbf{r}_u \rangle$, $F = \langle \mathbf{r}_u, \mathbf{r}_v \rangle$ and $G = \langle \mathbf{r}_v, \mathbf{r}_v \rangle$ denote the coefficients of the first fundamental form of S at the considered point $\mathbf{r}(u, v)$.

3.2 Building $V(P)$

$V(P)$ is calculated employing a divide and conquer scheme, i.e. by dividing the set P in two subsets L and R of approximately equal size, recursively calculating $V(L)$ and $V(R)$ and “sewing” these back together. In C-like pseudo code:

```
Voronoi diagram compute_voronoi( $P$  : Set of points) {
     $L, R$  : Sets of points;
     $V(L), V(R)$  : Voronoi diagrams;
    if( $|P| \leq 1$ ) {
        return  $\emptyset$ ;
    } else if( $|P| == 2$ ) {
        return medial curve of  $p_1$  and  $p_2$ ;
    } else {
        divide  $P$  into sets  $L$  and  $R$  of roughly equal size;
         $V(L) = \text{compute\_voronoi}(L)$ ;
         $V(R) = \text{compute\_voronoi}(R)$ ;
        return merge_subdiagrams( $V(L), V(R)$ );
    }
}
```

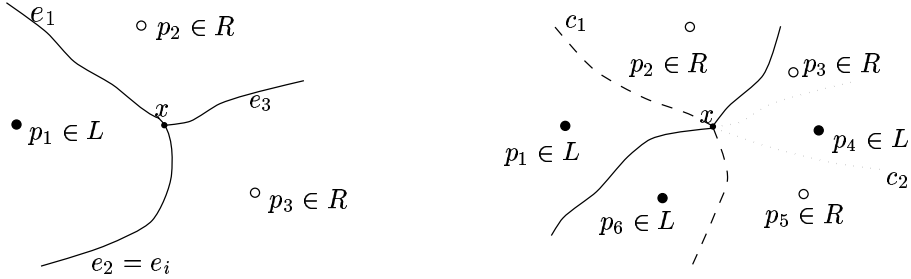


Figure 1: Bisecting edges at a Voronoi vertex

Subdivision of P in two disjunct subsets L and R can easily be achieved by dividing the parameter domain of S along a straight vertical or horizontal line. Computing the medial curve of two points can be accomplished employing the tools described above. The main difficulty lies in `merge_subdiagrams`, where we have to find those edges of $V(P)$ which are neither part of $V(L)$ nor $V(R)$.

Definition 3.7 Let P be a finite set of points, and $L, R \subset P$ a partition of P . A region of $D(p, P)$ as defined in (1) is called **L -region** or **R -region** if $p \in L$ or $p \in R$ respectively. An edge $e \in V(P)$ is called **L -edge** if it is the common border of two L -regions, **R -edge** if it borders two R -regions and **bisecting edge** if it is the common border of both a L - and a R -region.

The **bisector of L and R (with respect to P)** is the set of all bisecting edges $e \in V(P)$.

We will now discuss some properties of the bisector.

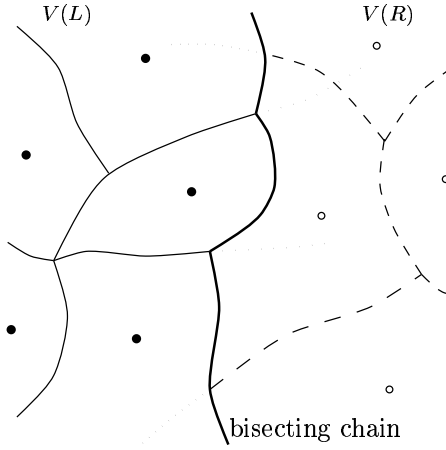
Proposition 3.8 The bisector of L and R consists of finitely many chains of consecutive edges; we will call these **bisecting chains**. Each bisecting chain either starts and ends at the border of the parameter domain of S or is a closed curve within the parameter domain.

Proof: Since the bisector consists of edges of $V(P)$ and there are only finitely many of these the first claim is obvious. As for the second claim, let e_1 be a bisecting edge and x a terminal point of e_1 . Since e_1 is a Voronoi edge, x must be either a border point of the parameter domain of S or a Voronoi vertex. In the latter case, the set $E := \{e_i \in V(P) | e_{-i} \cap e_1 = x\}$ of Voronoi edges incident with x consists of at least two elements. By assumption, e_1 is the common border of both a L - and a R -region. Thus there is at least one other bisecting edge $e_i \in E$ continuing the bisecting chain; see left half of figure 1 for an illustration. This shows that every bisecting chain either terminates at the border of the parameter domain of S or is a closed curve. ■

Note that two or more bisecting chains can meet at a Voronoi vertex, see right half of figure 1.

Definition 3.9 Let λ be the (straight) line in the parameter domain of S used to divide P into the subsets L and R . A Voronoi region $D(p, X)$, $X \in \{L, R\}$ is called an **outer region** if $\lambda \cap \overline{D(p, X)} \neq \emptyset$. All other regions are called **inner regions**.

Proposition 3.10 Let $p \in L$, $q \in R$. If both $D(p, L)$ and $D(q, R)$ are inner regions there exists no bisecting edge $e_{p,q} \in V(P)$.

Figure 2: Merging $V(L)$ and $V(R)$

Proof: It is obvious from definition (1) that $\overline{D(p, L)} \supset \overline{D(p, P)}$ and $\overline{D(q, R)} \supset \overline{D(q, P)}$. Since $e_{p,q} \subset \overline{D(p, P)} \cap \overline{D(q, P)} \subset \overline{D(p, L)} \cap \overline{D(q, R)}$ the proposition follows immediately from $\overline{D(p, L)} \cap \overline{D(q, R)} = \emptyset$ ■

According to proposition 3.10 we can limit our search for starting points of bisecting edges to the outer regions of L and R . Since we assumed every Voronoi edge to start and end at a Voronoi vertex, it is sufficient to scan the borders of these outer regions for starting points of bisecting edges. Note that the border of an outer domain needs not to consist entirely of Voronoi edges, it may include parts of the boundary of the parameter domain of S , if the region extends to this boundary.

Scanning edges for Voronoi vertices is not as difficult as it may seem: Since the Voronoi regions $\{D(p, R) | p \in R\}$ together with the edges $\{e | e \in V(R)\}$ form a partition of the parameter space of S , every point z in the parameter domain of S and thus every point on an edge $e \in V(L)$ belongs to exactly one Voronoi region $D(p, R)$ if it is not part of an edge $f \in V(R)$. If $z \in f$ and z is no Voronoi vertex of $V(R)$, there are exactly two points $p_1, p_2 \in R$ with $z \in \overline{D(p_i, R)}$. Even if z is a Voronoi vertex of $V(R)$, we know which points are centers of regions incident with this point. Thus we know exactly which regions $D(p, R)$, $p \in R$ can possibly be incident with a Voronoi vertex on e . The same argument applies to edges of $V(R)$.

By scanning the border of outer regions of $V(L)$ and $V(R)$ for these Voronoi vertices, we obtain starting points for tracing the bisecting edges. Note however that these may not be all new Voronoi vertices: We scan outer edges only for starting points, but bisecting edges may start or end on edges of inner regions. However these belong to a bisecting chain starting and ending at points on edges of outer regions or on the boundary of the parameter domain.

The remaining problems we have to solve is how to trim edges of $V(L)$ and $V(R)$ at those new Voronoi vertices, and how to continue tracing in case this edge does not belong to an outer region. This problem however is well researched, see e.g. [7] for the Euclidean case and [4] for abstract Voronoi diagrams. All in all, we get this algorithm for merging the sub-diagrams $V(L)$ and $V(R)$:

```

Voronoi diagram merge_subdiagrams( $V(L)$ ,  $V(R)$  : Voronoi diagrams) {
     $P$  : Set of starting points of bisecting edges;
     $V(P)$  : Voronoi diagram;
     $e$  : Voronoi edge;
     $v$  : Voronoi vertex;
     $i$  : integer;
     $P = \{ \text{starting points on borders of outer regions of } V(R) \} \cup \{ \text{starting points on borders of outer regions of } V(L) \};$ 
     $V(P) = V(L) \cup V(R);$ 
     $i = 0;$ 
    while( $i < |P|$ ) {
         $i = i + 1;$ 
        for(every bisecting edge  $e$  starting at  $P_i$  and not marked as done) {
            trace  $e$  to its endpoint  $v$ ;
            trim edges of  $V(L)$  respective  $V(R)$  at  $P_i$ ;
            mark  $e$  as done at  $P_i$ ;
            while( $v \notin P$ ) {
                add  $e$  to  $V(P)$ ;
                trim edges of  $V(L)$  respective  $V(R)$  at  $v$ ;
                determine new edge  $e$  at  $v$ ;
                trace  $e$  to its endpoint  $v_e$ ;
                 $v = v_e;$ 
            }
            trim edges of  $V(L)$  respective  $V(R)$  at  $v$ ;
            add  $e$  to  $V(P)$ ;
            mark  $e$  as done at  $v$ ;
        }
    }
}

```

4 Results

With aid of the tools developed in section 3, we are able to compute Voronoi diagrams on parameterized surfaces. As of now, we have implemented the algorithm described above in C++. It can be shown that we indeed compute correct geodesic Voronoi diagrams due to the fact that geodesics emanating from the center p of a Voronoi region $D(p, P)$ stay distance minimal until they reach the border of $D(p, P)$ provided they do not contain conjugate points of p , i.e. points where $\partial_t \mathcal{O}_p$ vanishes, and the border of $D(p, P)$ has no self-intersections (c.f. [10, 8, 9] for background on distance minimal geodesics). In computing the Voronoi edges, we check that both of these conditions are fulfilled. First numerical experiments have shown our algorithm to be numerically stable and to trace Voronoi edges with quite high accuracy. By solving the differential equations (13) it appears to be possible to determine points on the Voronoi edge with a position accuracy of 10^{-12} provided all calculations are done in double precision.

Some small examples of geodesic Voronoi diagrams are shown here: Figure 3 shows a geodesic Voronoi diagram on a wave-like surface given by $\mathbf{r}(u, v) = (u, v, \sin u \cos v)$ and the corresponding curves in parameter space, figure 4 shows a geodesic Voronoi diagram on a paraboloid parameterized by $\mathbf{r}(u, v) = (u, v, u^2 + v^2)$ along with corresponding curves in parameter space.

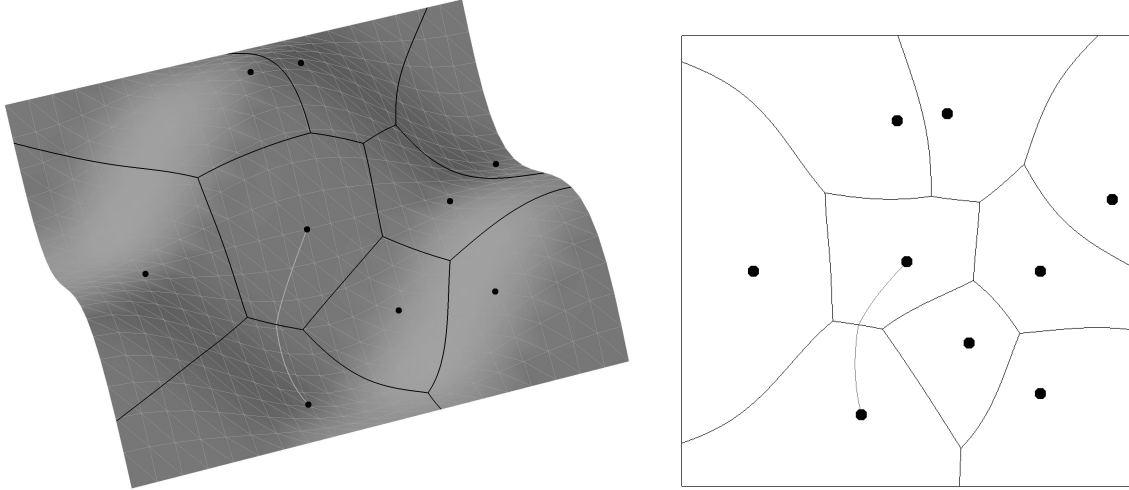


Figure 3: Voronoi diagram on a wave-like surface and corresponding curves in parameter space. A pair of geodesics connecting the centers of two Voronoi regions with a point on their common Voronoi edge is drawn for illustration.

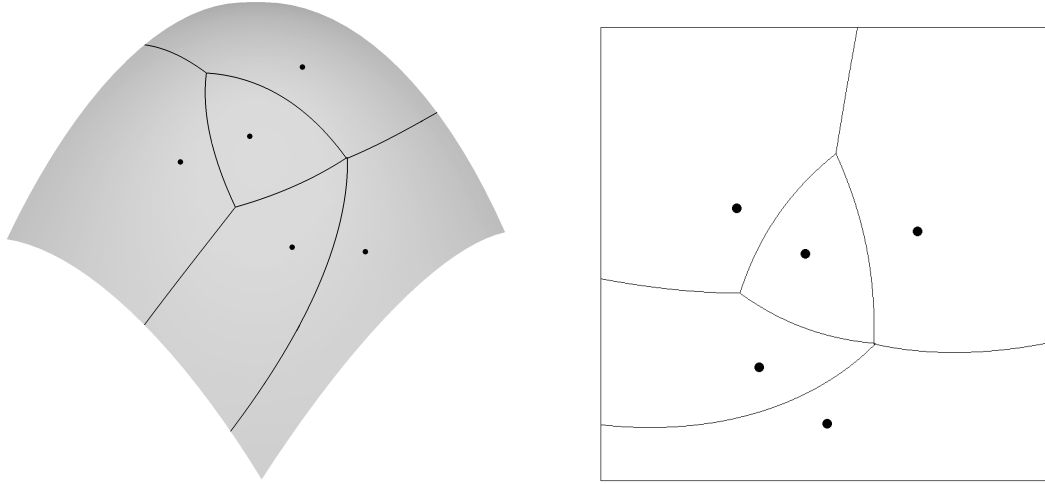


Figure 4: Voronoi diagram on a paraboloid and corresponding curves in parameter space

These two examples indicate another result shown more clearly in figure 5: Even if these geodesic Voronoi diagrams are topologically the same as Euclidean Voronoi diagrams of the same set of points, they are analytically quite different. Figure 6 shows that geodesic Voronoi diagrams may not even be topologically equivalent to Euclidean Voronoi diagrams of the same set of points.

In section 2.2, we required that each Voronoi edge start at either a Voronoi vertex or the boundary of the parameter space of S . This assumption holds for surface patches S which are “reasonably similar” to a plane, but as sketched in figure 6 there are quite a few surfaces where this assumption does not hold. We are working on a method to lift this restraint, allowing us to calculate Voronoi diagrams where one region “floods” part of the diagram, creating “island regions”.

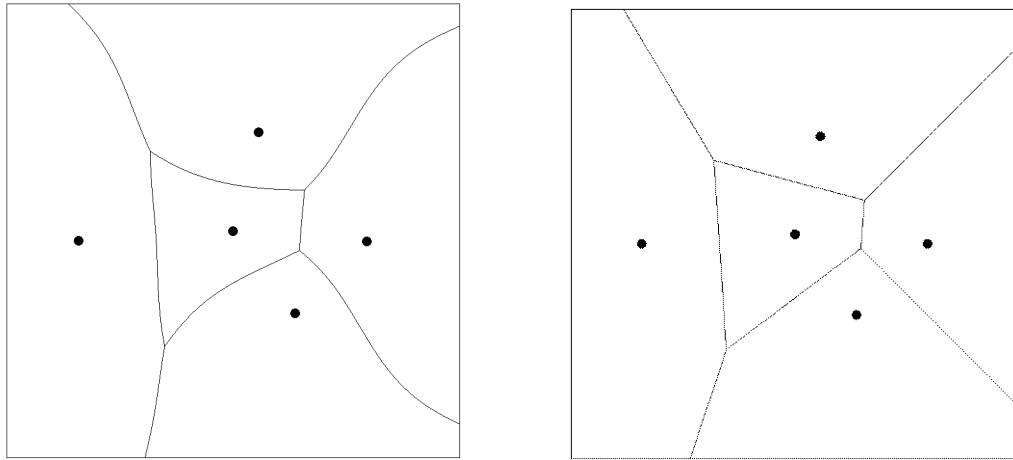


Figure 5: Geodesic Voronoi diagram of five points on a wave-like surface and Euclidean Voronoi diagram of the same set of points

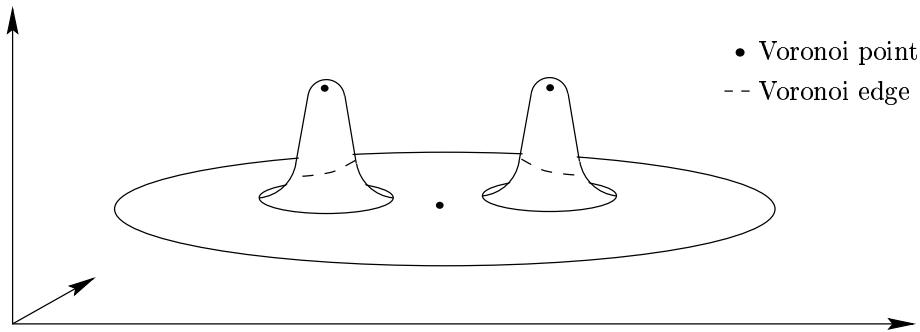


Figure 6: Sketch of a Voronoi diagram with three points and two “islands”

References

- [1] F. Aurenhammer. Voronoi diagrams - a survey of a fundamental geometric data structure. *ACM Computing Surveys*, 23(3):245–405, September 1991.
- [2] W. Blaschke and K. Leichtweiss. *Elementare Differentialgeometrie*. Springer-Verlag, Berlin, 1973.
- [3] M. P. do Carmo. *Differential Geometry of Curves and Surfaces*. Prentice Hall, Inc., Englewood Cliffs, New Jersey, 1976.
- [4] R. Klein. *Concrete and Abstract Voronoi Diagrams*. Lecture Notes in Computer Science. Springer, Berlin Heidelberg New York, 1st edition, 1989.
- [5] T. Maekawa. Computation of shortest paths on parametric free-form surfaces. *Journal of Mechanical Design, ASME Transactions* 118 (4), pages 499–508, 1996.
- [6] T. Rausch, F.-E. Wolter, and O. Sniehotta. Computation of medial curves on surfaces. *Welfen laboratory report*, (1), August 1996.
- [7] M. I. Shamos and D. Hoey. Closest-point problems. *Proceedings of the 16th Annual IEEE Symposium on FOCS*, pages 151–162, 1975.
- [8] F.-E. Wolter. Distance function and cut loci on a complete riemannian manifold. *Archiv der Mathematik*, 32:92–96, 1979.
- [9] F.-E. Wolter. Interior metric, shortest paths and loops in riemannian manifolds with not necessarily smooth boundary. *Diploma Thesis, Freie Univ. Berlin*, 1979.
- [10] F.-E. Wolter. *Cut Loci in Bordered and Unbordered Riemannian Manifolds*. PhD thesis, Technical University of Berlin, Department of Mathematics, December 1985.